SUPPORTING INFORMATION

Terpenes, natural dyes and photochemistry: toward the synthesis of photoactive bio-based materials with biocide properties

L. Breloy,[a] C. Elian,[a] S. Abbad Andaloussi,[b] S. Lajnef,[c] F. Peyrot,[c,d] D. L. Versace[a]*

[a] Univ Paris Est Creteil, CNRS, ICMPE, UMR 7182, 2 rue Henri Dunant, 94320 Thiais, France.

[b] Laboratoire Eau, Environnement, Systemes Urbains (LEESU), UMR-MA 102, Universite Paris-Est Creteil (UPEC), 61 Avenue Genéral de Gaulle, 94010 Créteil Cedex, France.

[c] Université Paris Cité, CNRS, Laboratoire de Chimie et Biochimie Pharmacologiques et Toxicologiques, F-75006 Paris, France

[d] Sorbonne-Université, Institut National Supérieur du Professorat et de l'Education (INSPE) de l'Académie de Paris, F-75016 Paris, France

*Corresponding author: davy-louis.versace@u-pec.fr

TABLES

Table S1. Final IR conversions of TT thiol groups and geraniol ene groups in TT/Ger blend mixture with different ratios (25%/75%, 33%/67% and 50%/50% w/w) under air in the presence of Al-2Ac and P-3Ac under LED@405 nm, 455 nm and 470 nm after 800 s. [PS] = 0.5 wt%. PS = Al-2Ac and P-3Ac.

		405 nm	455 nm	470 nm
Al-2Ac/TT25%/Ger75%	SH	nm	nm	nm
	Ene			
Al-2Ac/TT33%/Ger67%	SH	70%	nm	nm
	Ene	46%		
Al-2Ac/TT50%/Ger50%	SH	56%	nm	nm
	Ene	68%		
P-3Ac/TT25%/Ger75%	SH	87%	56%	nm
	Ene	53%	43%	
P-3Ac/TT33%/Ger67%	SH	86%	74%	nm
	Ene	67%	34%	
P-3Ac/TT50%/Ger50%	SH	52%	nm	nm
	Ene	61%		

nm: non-measurable with our experimental setting, as the conversions were too low to ensure the retention of the liquid on the BaF_2 pellet.

Table S2. Average contact angles at the surface of P-3Ac/TT/Lin/SOA and P-3Ac/TT/SOA materials. Average within 3 samples.

Materials	**Contact angle (°)**
P-3Ac/TT/Lin/SOA	60.9 ± 0.6
P-3Ac/TT/SOA	80.7 ± 1.7

SCHEMES

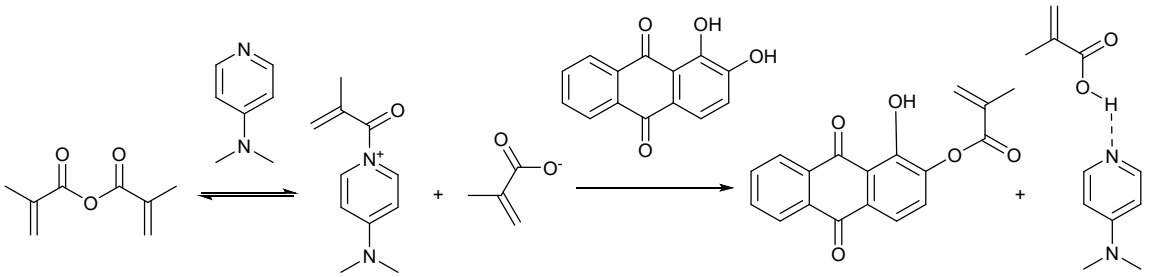

Scheme S1. Mechanism of DMAP-catalysed transesterification of alizarin by methacrylic anhydride.

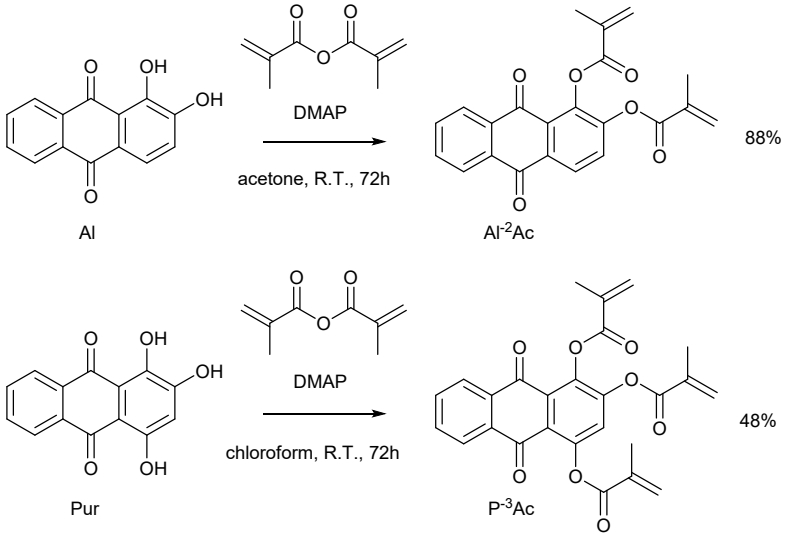

Scheme S2. Synthesis of the di-methacrylated alizarin (Al-2Ac) and the tri-methacrylated purpurin (P-3Ac).

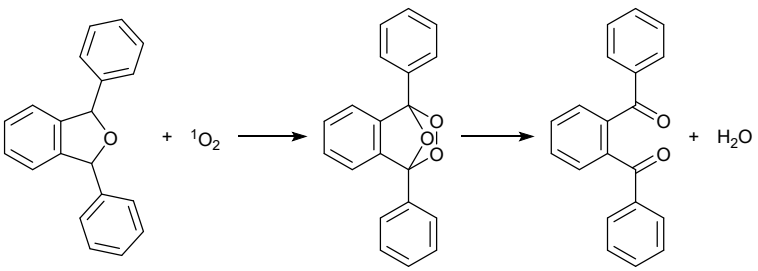

Scheme S3. DPBF reaction with singlet oxygen.

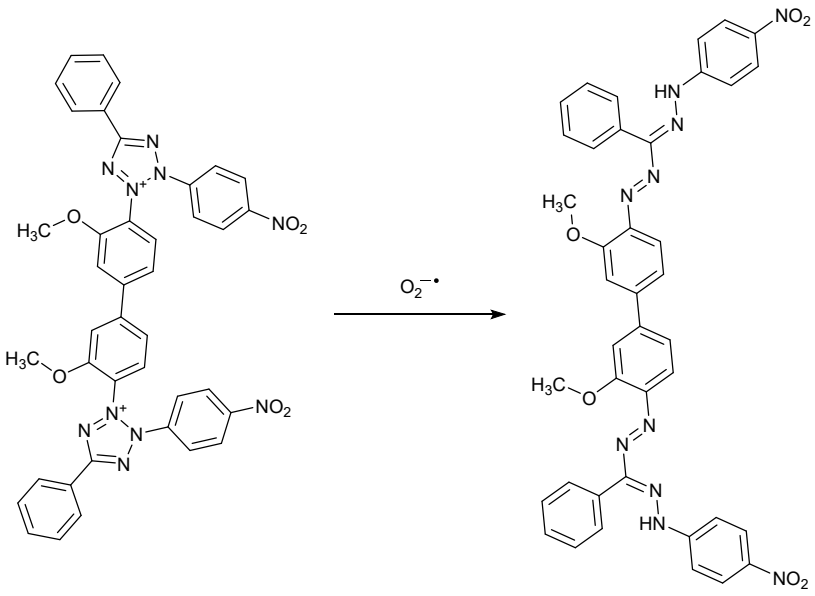

Scheme S4. NB reaction with superoxide anion.

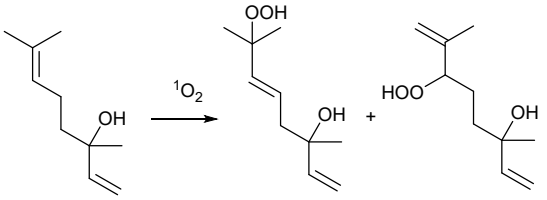

Scheme S5. Reaction of linalool with singlet oxygen.[1]

FIGURES

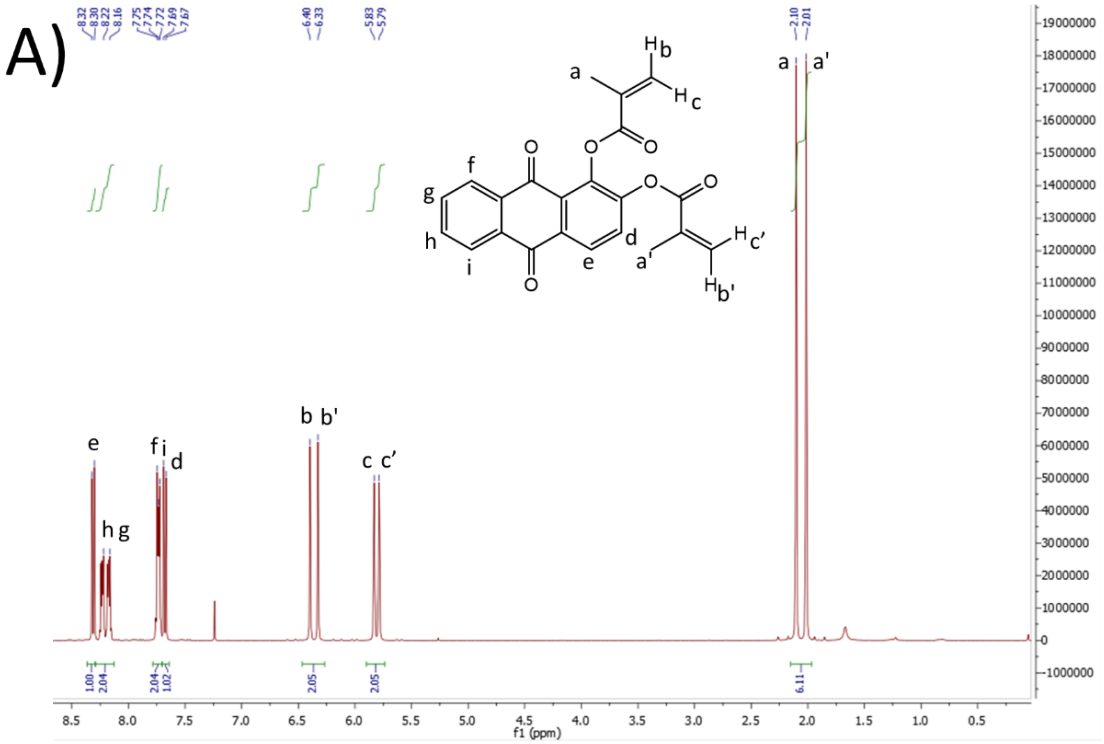

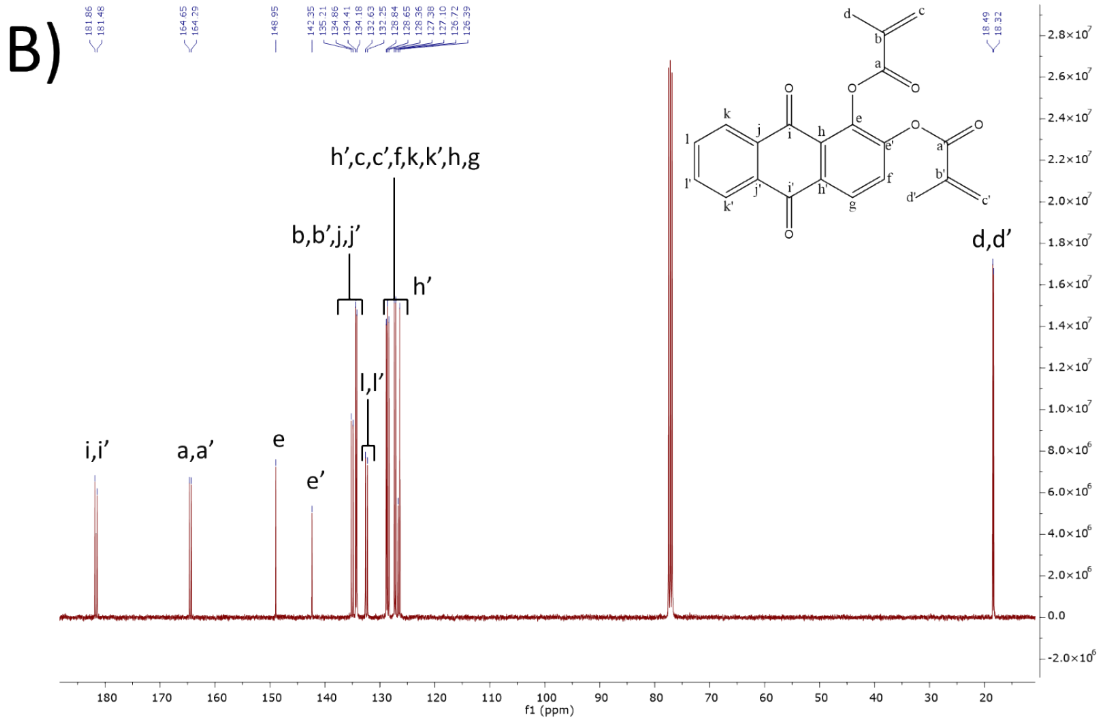

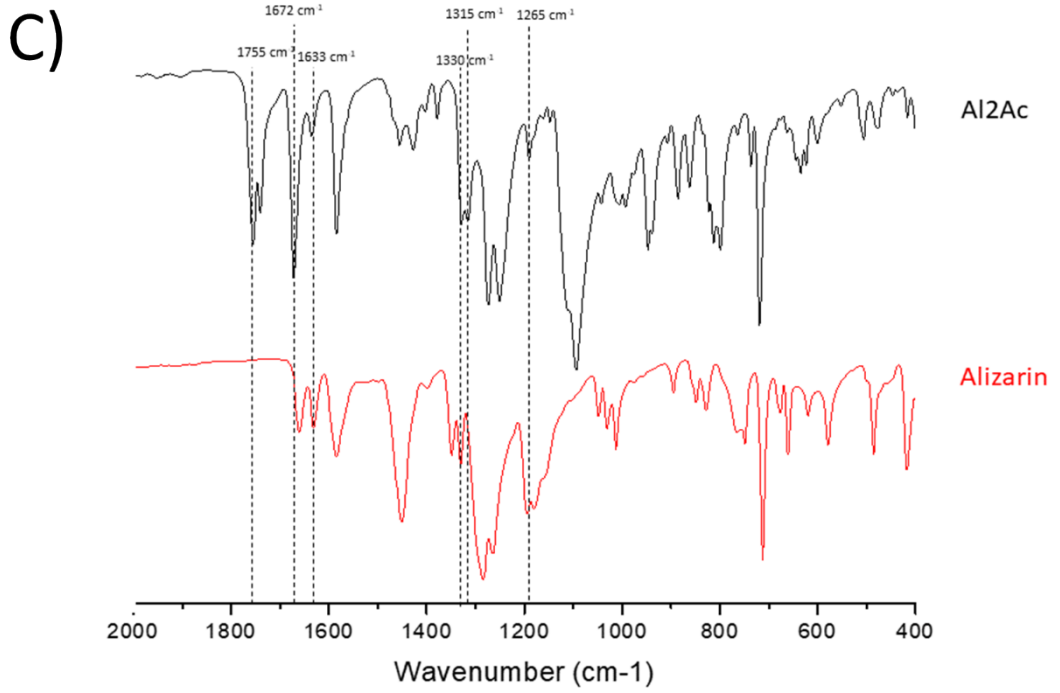

Figure S1. Characterization of Al-2Ac: (A) ^{1}H NMR, (B) ^{13}C NMR, and (C) IR spectra compared to native and non-modified alizarin.

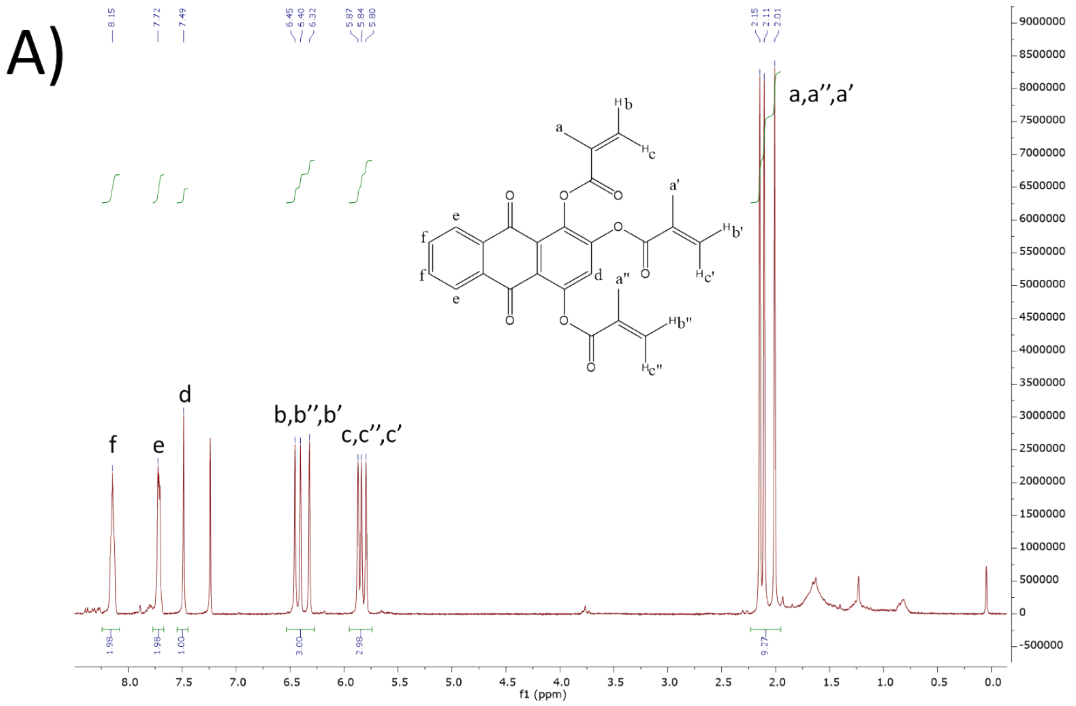

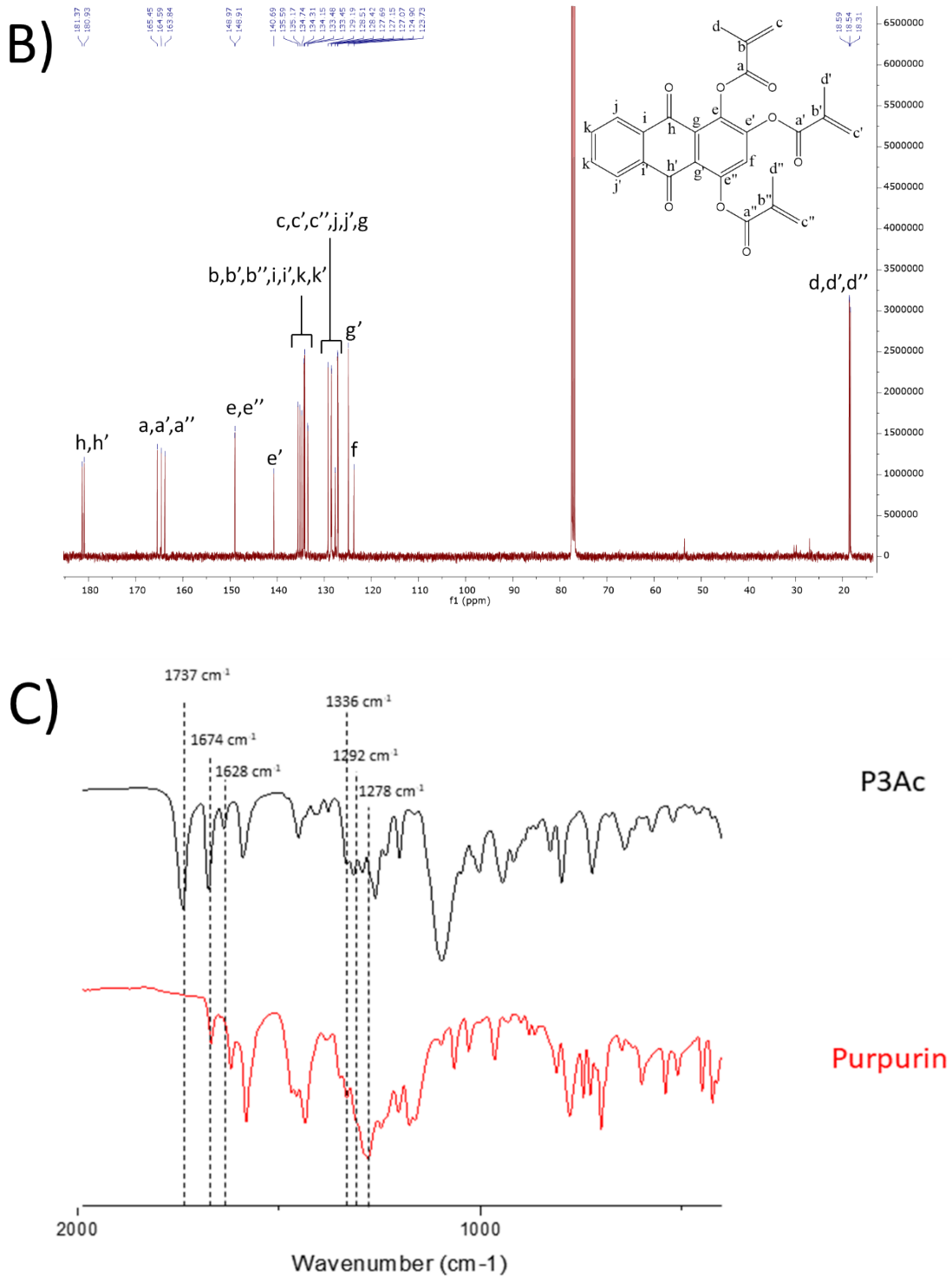

Figure S2. Characterization of P-3Ac: (A) ^{1}H NMR, (B) ^{13}C NMR and (C) IR spectra compared to native and non-modified purpurin.

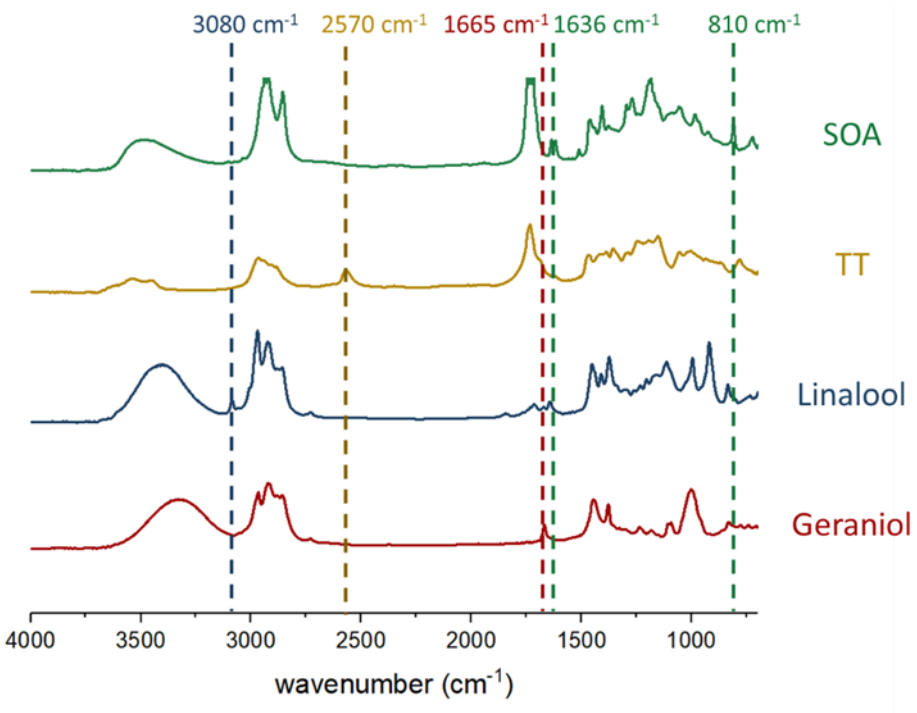

Figure S3. Stacking of IR spectra of the studied monomers.

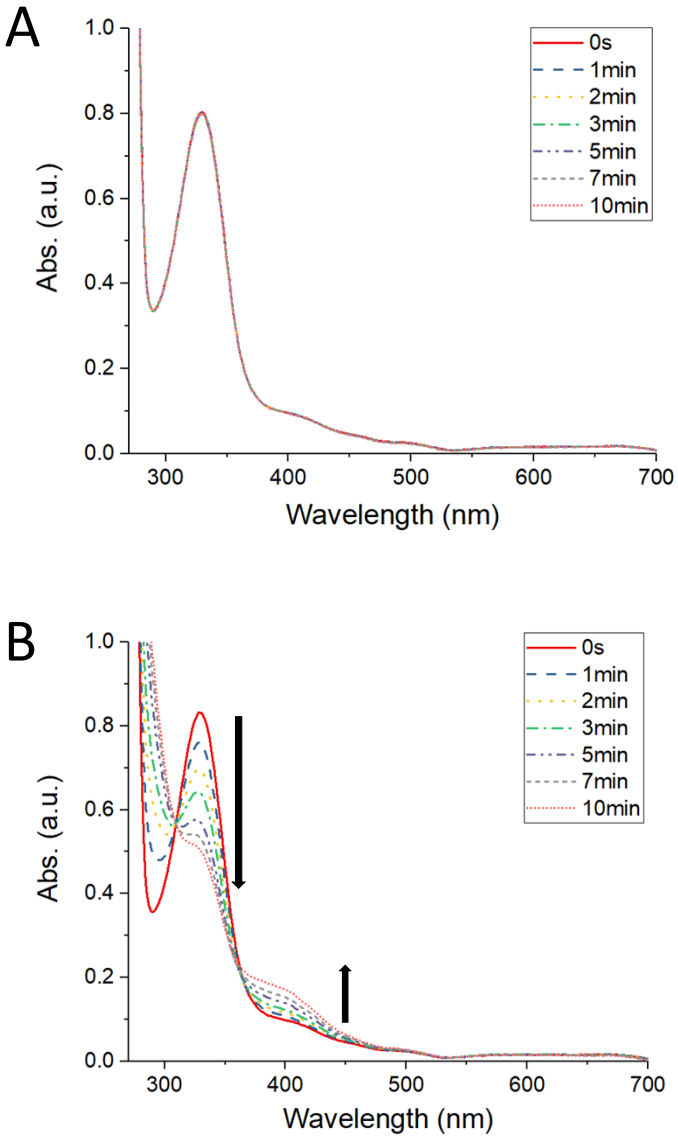

Figure S4. Steady-state photolysis of Al-2Ac ([Al-2Ac] = 1.4 x 10^{-4} M) in ACN under LED@405 nm (60 mW/cm^2) (A) alone and in the presence of (B) TT ([TT] = 2.4 x 10^{-3} M)

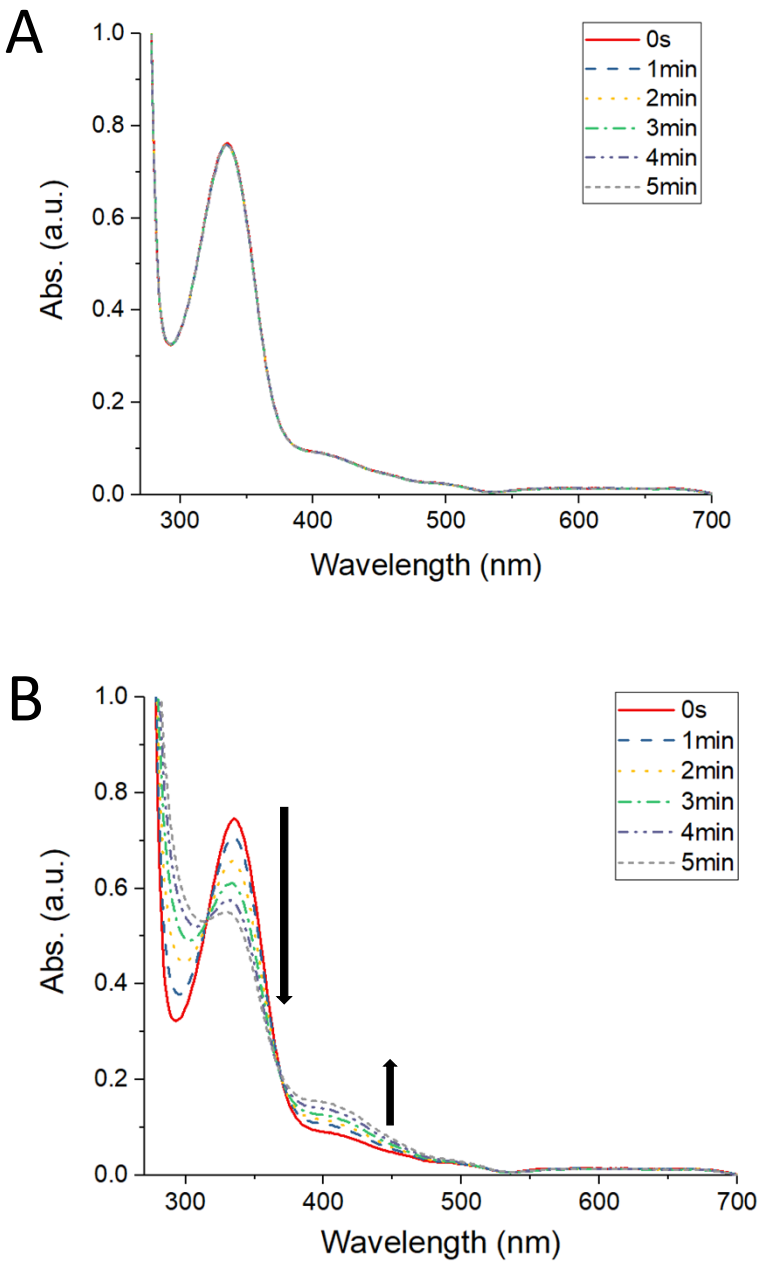

Figure S5. Steady-state photolysis of P-3Ac ([P-3Ac] = 1.2 x 10^{-4} M) in ACN under LED@405nm (60 mW/cm^2) (A) alone and in the presence of (B) TT ([TT] = 2.4 x 10^{-3} M)

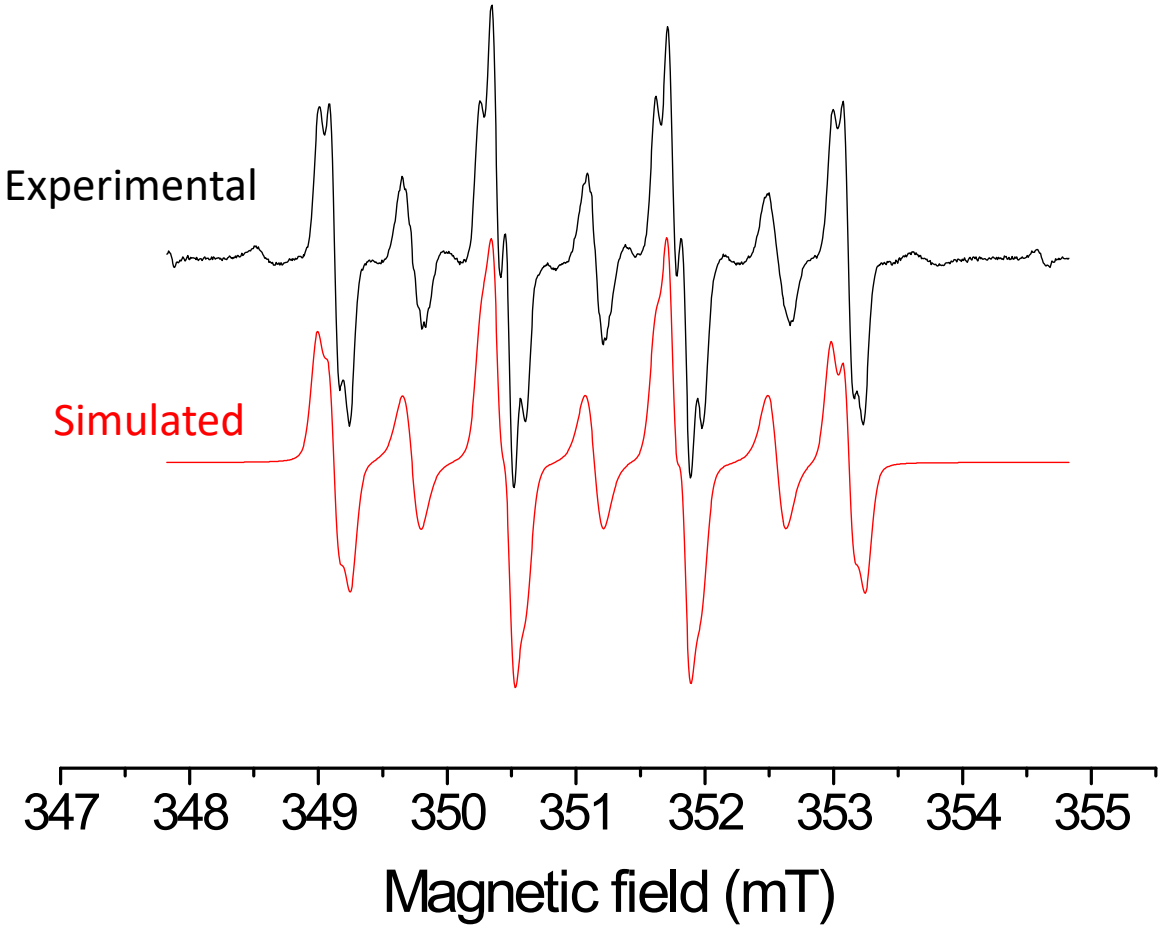

Figure S6. The normalized experimental and simulated ESR ST spectra obtained in DCM under argon during 120-s ex situ LED@405 nm irradiation of Al-2Ac/TT/DMPO. Intensity of irradiation = 60 mW/cm^2. Only two species (I and II, scheme 2) were considered in the simulation.

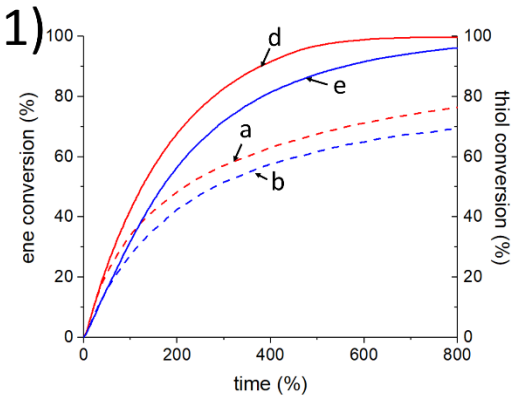
1)
ene conversion (%)
thiol conversion (%)
time (%)
a
b
d
e

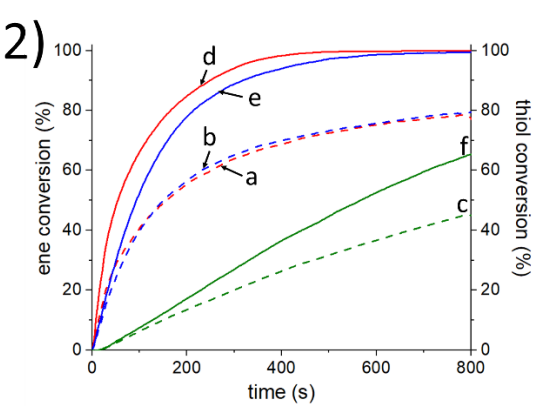
2)
ene conversion (%)
thiol conversion (%)
time (s)
a
b
c
d
e
f

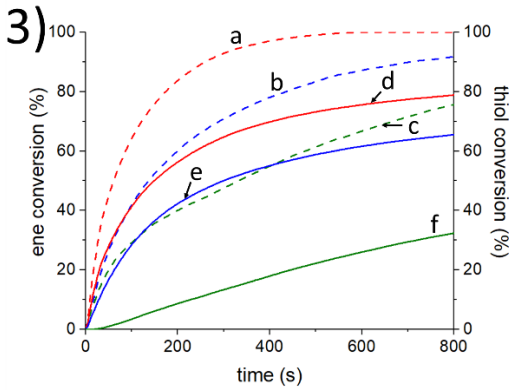
3)
ene conversion (%)
thiol conversion (%)
time (s)
a
b
c
d
e
f

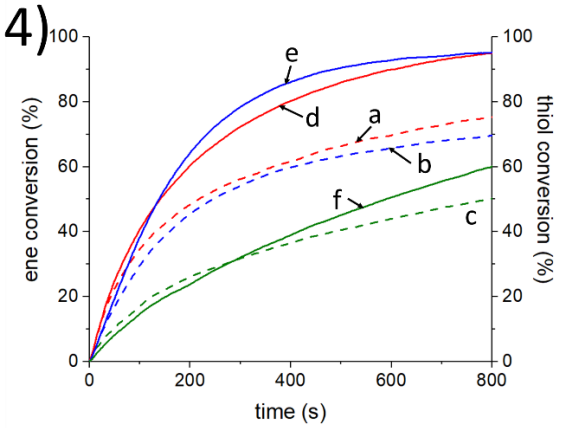
4)
ene conversion (%)
thiol conversion (%)
time (s)
a
b
c
d
e
f

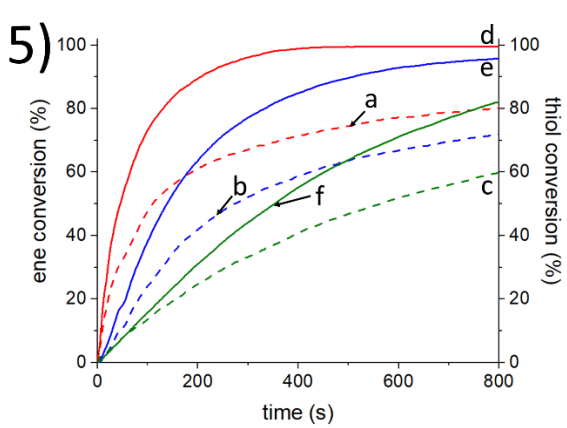
5)
ene conversion (%)
thiol conversion (%)
time (s)
a
b
c
d
e
f

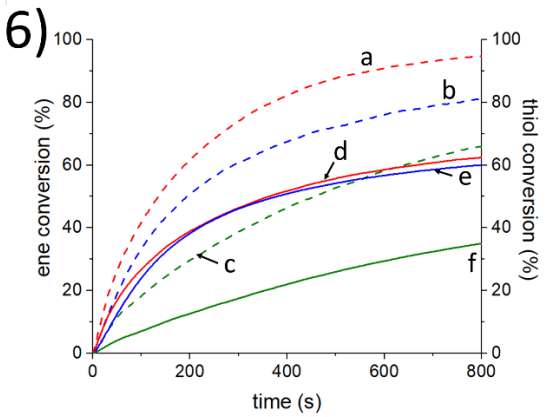
6)
ene conversion (%)
thiol conversion (%)
time (s)
a
b
c
d
e
f

Figure S7. Kinetic profiles of ene and thiol conversions under air in (1) Al-2Ac/TT25%/Lin75%, (2) Al-2Ac/TT33%/Lin67% (3) Al-2Ac/TT50%/Lin50%, (4) P-3Ac/TT25%/Lin75%, P-3Ac/TT33%/Lin67% and (6) P-3Ac/TT50%/Lin50%: ene conversion (---) upon (a) LED@405 nm, (b) LED@455 nm and (c) LED@470 nm; and thiol conversion (—) upon (d) LED@405 nm, (e) LED@455 nm and (f) LED@470 nm. [PI] = 0.5 wt%.

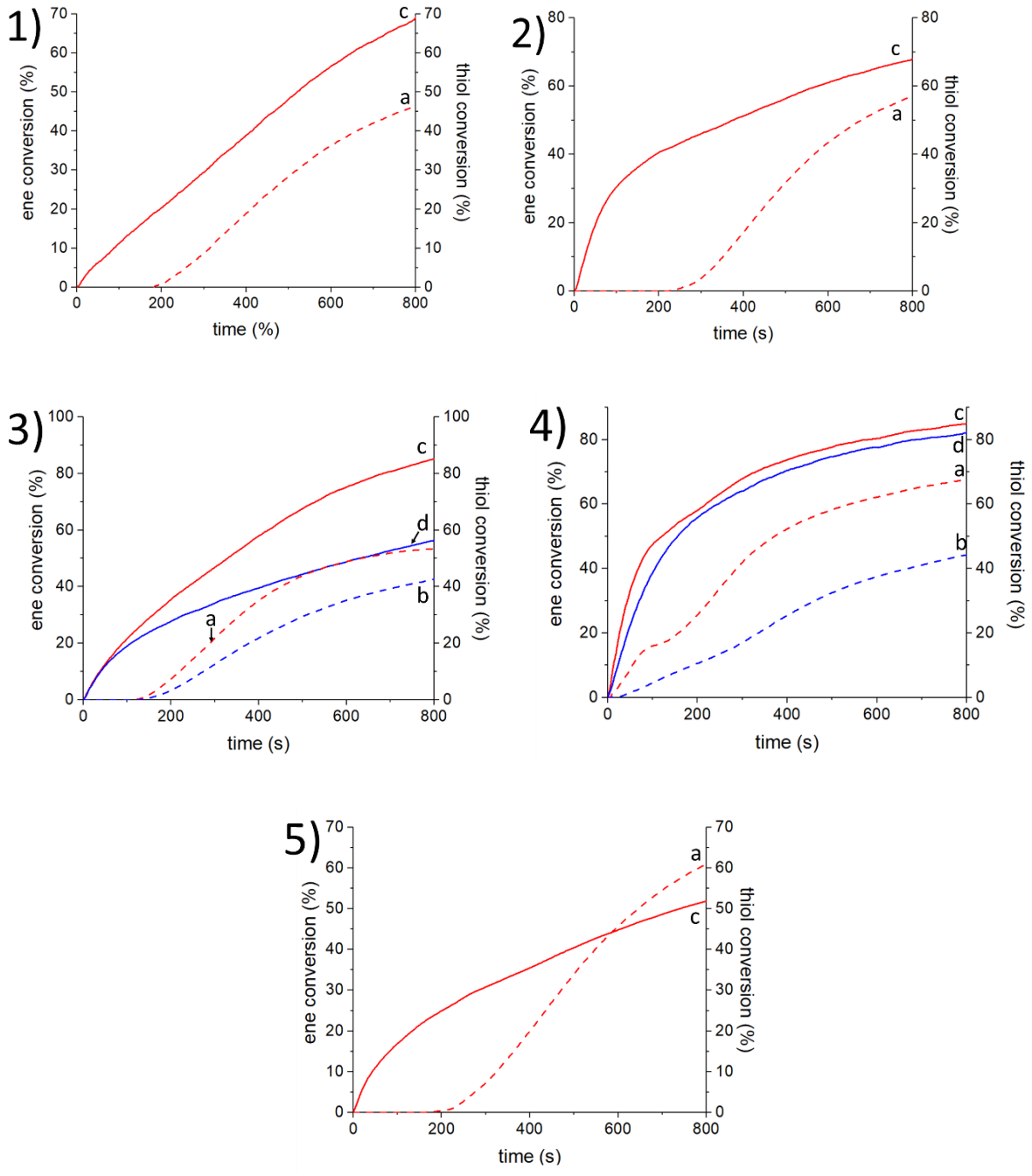

Figure S8. Kinetic profiles of ene and thiol conversions under air in (1) Al-2Ac/TT33%/Ger67%, (2) Al-2Ac/TT50%/Ger50%, (3) P-3Ac/TT25%/Ger75%, (4) P-

3Ac/TT33%/Ger67% and (5) P-3Ac/TT50%/Ger50%: ene conversion (---) upon (a) LED@405 nm and (b) LED@455 nm; and thiol conversion (—) upon (c) LED@405 nm and (d) LED@455 nm. [PI] = 0.5 wt%

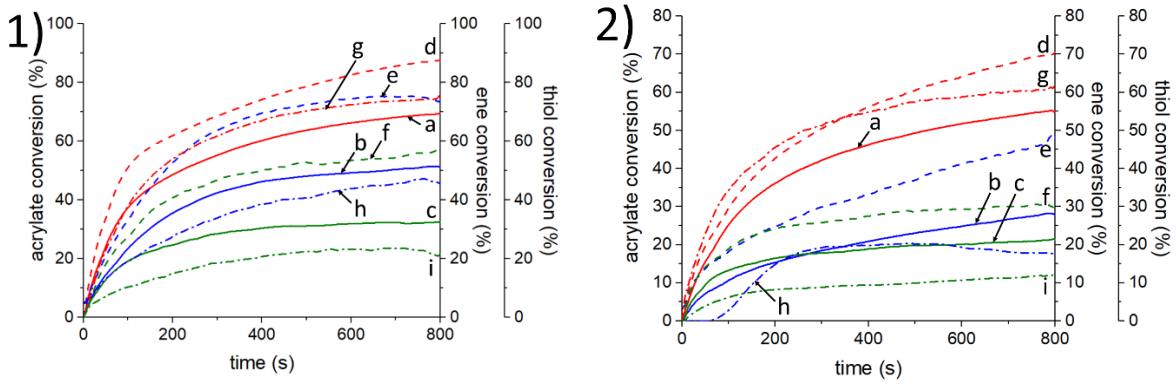

Figure S9. Kinetic profiles of monomer conversions in (1) Al/ TT25%/Lin25%/SOA50% and (2) Pur/TT25%/Lin25%/SOA50% systems in laminate: thiol conversion (—) upon (a) LED@405 nm, (b) LED@455 nm and (c) LED@470 nm; ene conversion (---) upon (d) LED@405 nm, (e) LED@455 nm and (f) LED@470 nm; and acrylate conversion (-·-) upon (g) LED@405 nm, (h) LED@455 nm and (i) LED@470 nm. [PI] = 0.5 wt%

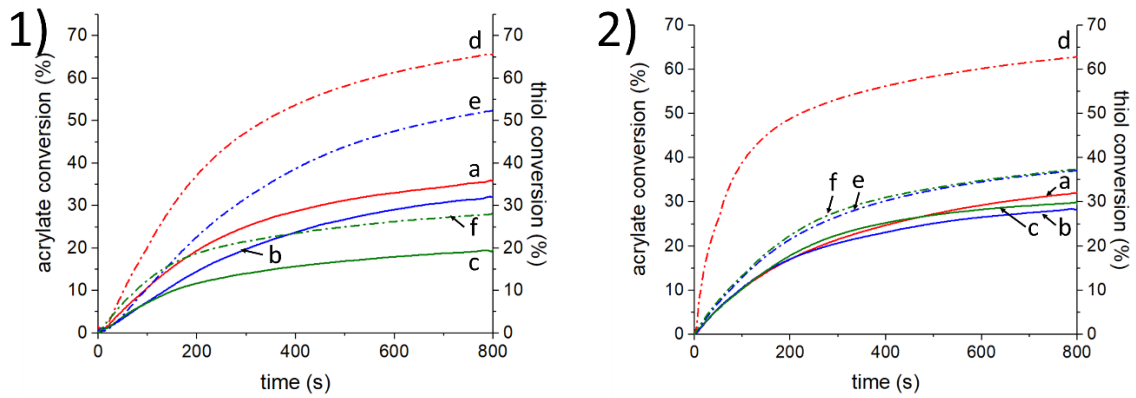

Figure S10. Kinetic profiles of acrylate and thiol conversions in (1) Al/TT25%/SOA75% and (2) Pur/TT25%/SOA75% in laminate: thiol conversion (—) upon (a) LED@405 nm, (b) LED@455 nm and (c) LED@470 nm; acrylate conversion (-·-) upon (d) LED@405 nm, (h) LED@455 nm and (i) LED@470 nm. [PI] = 0.5 wt%.

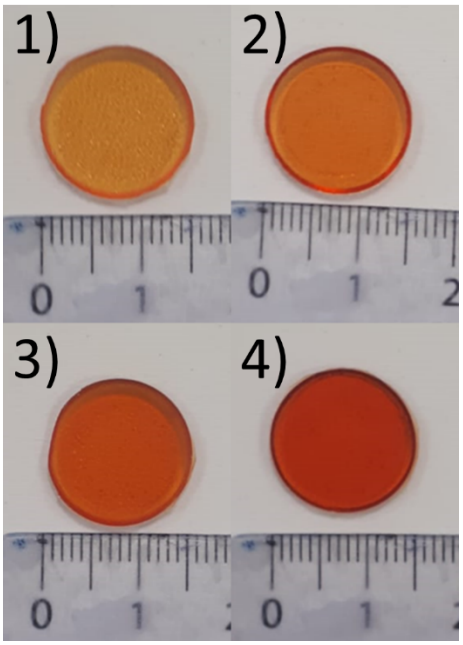

Figure S11. Optical images of (1) Al-2Ac/TT/Lin/SOA, (2) Al-2Ac/TT/SOA, (3) P-3Ac/TT/Lin/SOA and (4) P-3Ac/TT/SOA pellets generated under LED@405 nm irradiation.

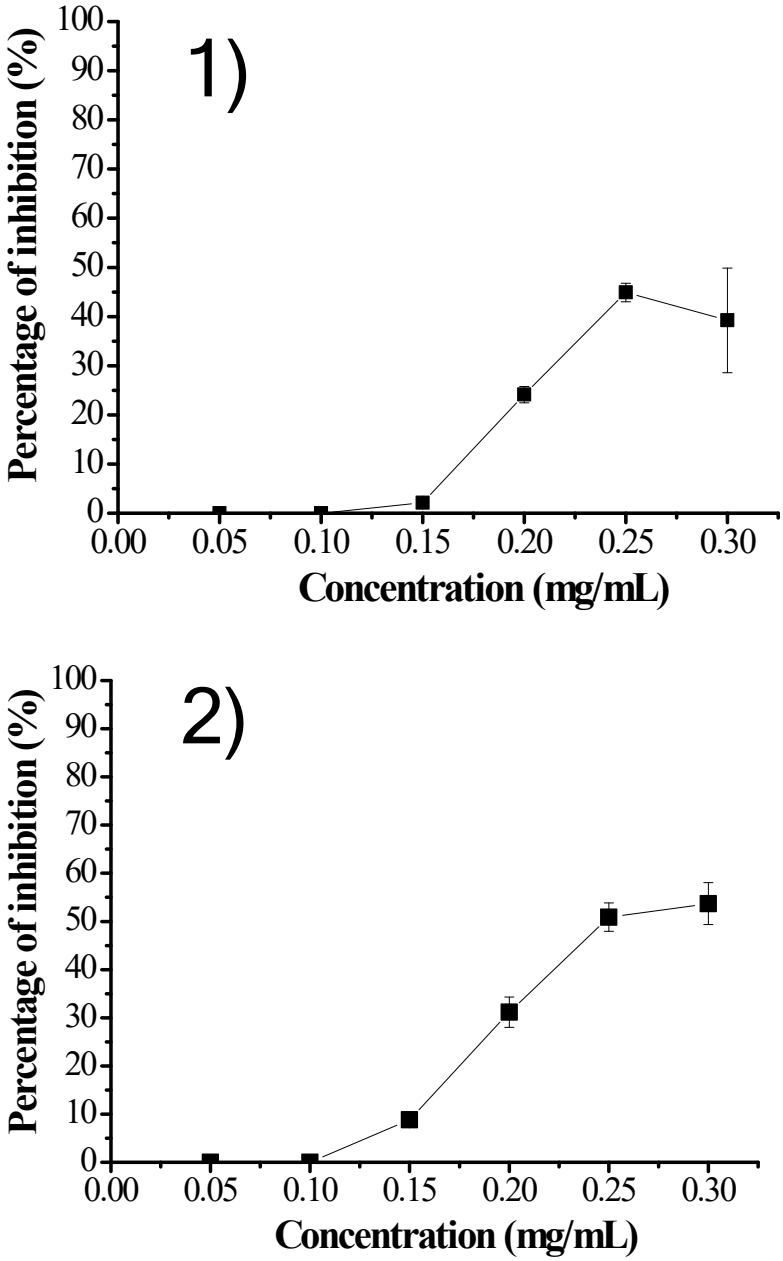

Figure S12. Percentage of inhibition of 1) *S. aureus* and 2) *E. coli* as a function of the concentration of P-3Ac.

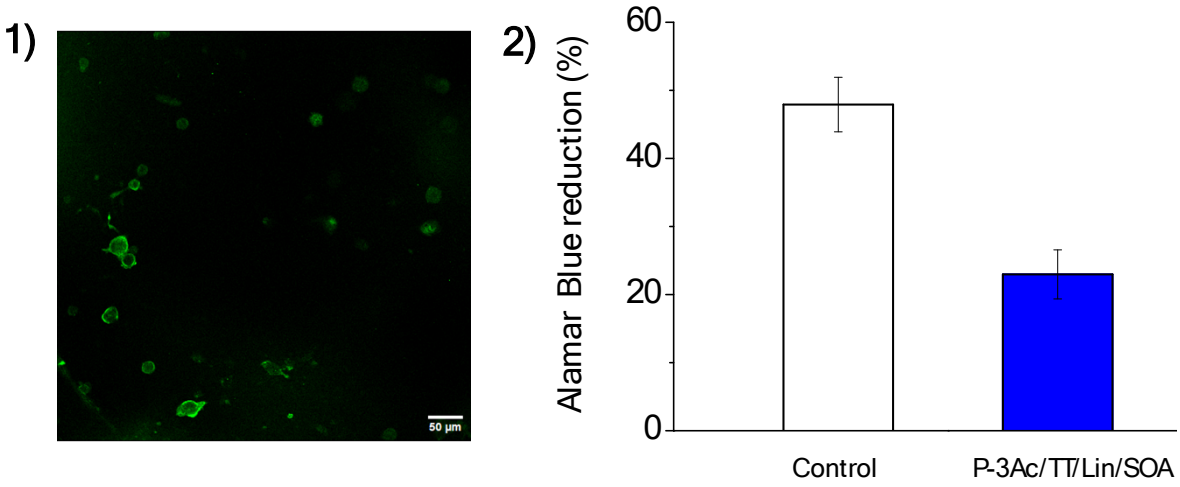

Figure S13. 1) NHDFs morphology on P-3Ac/TT25%/Lin25%/SOA50% disks after 24 h of culture. Cytoskeletons were stained with phalloidin (green fluorescence). Note the rounded morphology indicating poor cell adhesion. Scale bar: 50 µm; 2) Metabolic activity after 24 h, as assayed by the Alamar Blue reduction test, for NHDFs seeded on P-3Ac/TT25%/Lin25%/SOA50% (n=3) and in control polystyrene culture plate (n=3). Despite low cell density, metabolic activity was *ca*. 50 % that of the control.

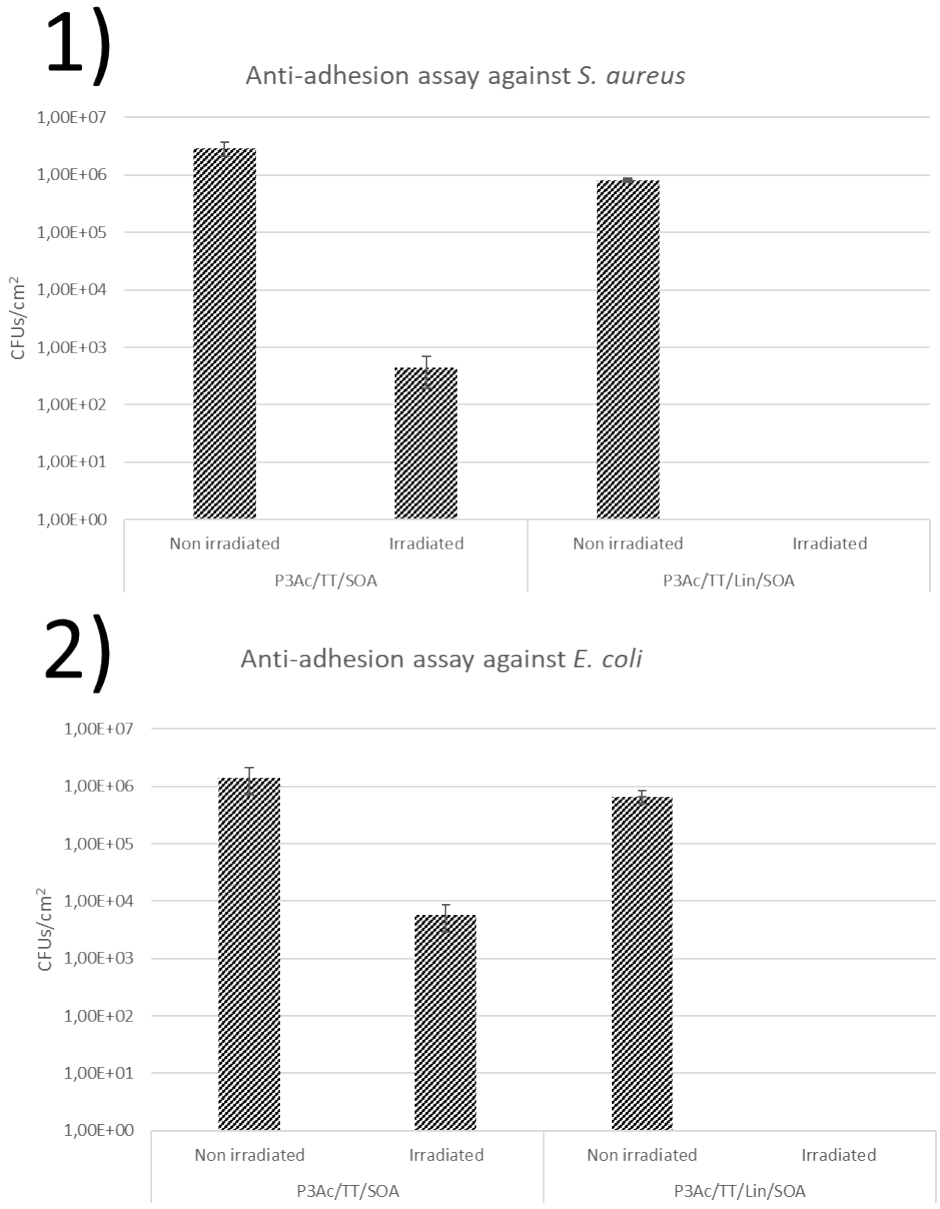

Figure S14. Evolution of the colony forming units (CFUs) of *S. aureus* (1) and *E. coli* (2) at the surface of the P-3Ac/TT/SOA and P-3Ac/TT/Lin/SOA materials which have been cleaned and reused. Antibacterial experiments with and without visible light by a solar emission lamp.

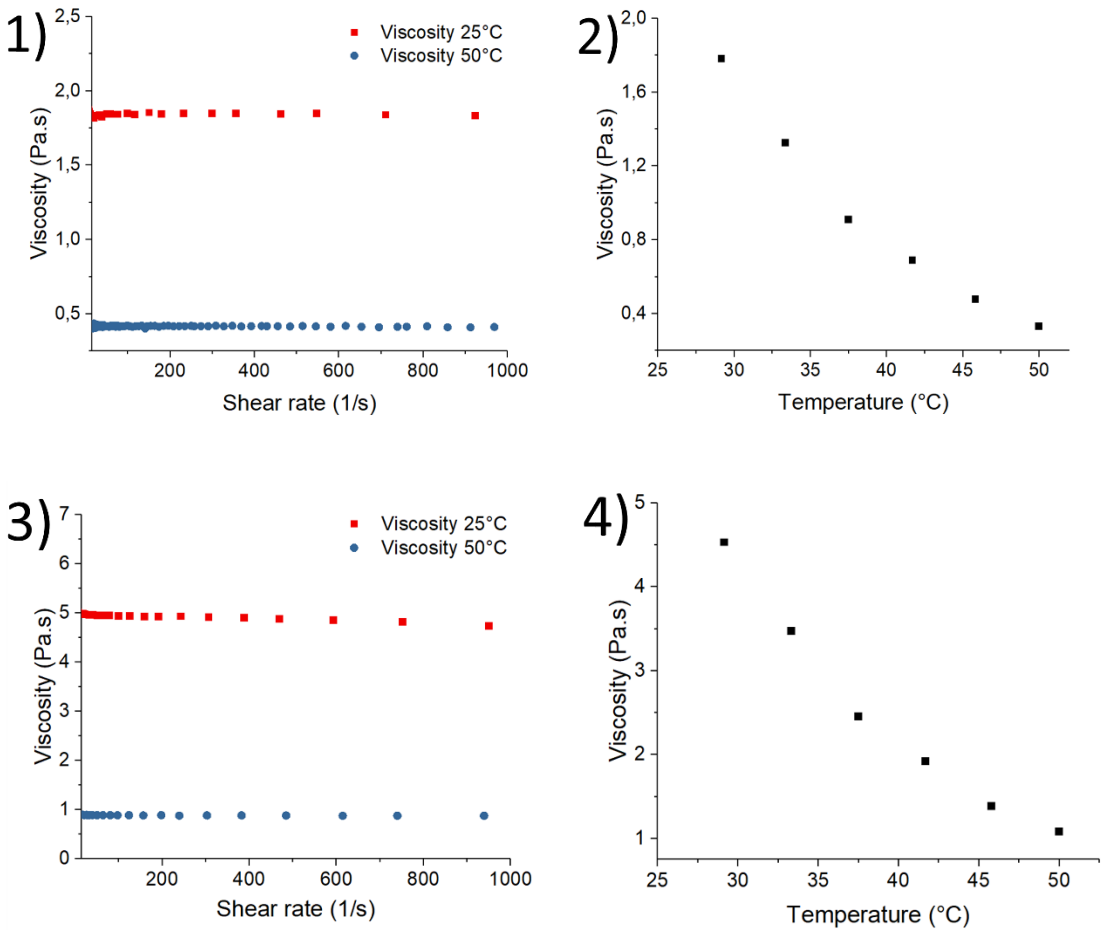

Figure S15. Evolution of viscosity over shear rate at 25°C and 50°C for (1) TT25%/Lin25%/SOA50% and (3) TT25%/SOA75%; and evolution of viscosity over temperature between 25°C and 50°C for (2) TT25%/Lin25%/SOA50% and (4) TT25%/SOA75%. Shear strain = 1 Hz, temperature ramp = 2°C.min^{-1}, 20-mm steel plate.

EQUATIONS

The bio-renewable carbon content (BCC) is an estimation of the amount of carbon present in the nature molecule over the total amount of carbon in the final monomer structure (natural molecule modified with polymerizable groups). For each formulation, the BCC was calculated as such:

$$\text{BCC (\%)} = 100 \times \frac{Bio - renewable\ carbon\ number}{Total\ carbon\ number\ in\ the\ monomer}$$

equation S1

With bio-renewable carbon number being the amount of carbon in the natural molecule (oil or terpene) from which the monomer is derived. The BCC of the polymerizable formulation is the sum of BCC monomers multiplied by their respective proportion in the mix.

For trithiol, the BCC is 0%, as the molecule as no obvious natural equivalent or origin.

For terpenes (linalool, geraniol, farnesene and myrcene), the BCC is 100%, as the natural molecule can be used as a monomer without further modification (natural occurrence of ene bounds).

REFERENCES

1. Elgendy, E. M.; Semeih, M. Y. Phyto – Monoterpene linalool as precursor to synthesis epoxides and hydroperoxides as anti carcinogenic agents via thermal and photo chemical oxidation reactions. *Arabian Journal of Chemistry* **2019,** 12 (7), 966-973 DOI: https://doi.org/10.1016/j.arabjc.2018.09.008.

2. Sautrot-Ba, P.; Brezová, V.; Malval, J.-P.; Chiappone, A.; Breloy, L.; Abbad-Andaloussi, S.; Versace, D.-L. Purpurin derivatives as visible-light photosensitizers for 3D printing and valuable biological applications, Polymer Chemistry 2021, 12, 2627-2642 DOI:10.1039/D1PY00126D